



Deposited via The University of Leeds.

White Rose Research Online URL for this paper:

<https://eprints.whiterose.ac.uk/id/eprint/142996/>

Version: Accepted Version

---

**Article:**

Sun, M, Feng, Y, Wall, P et al. (2019) On-line power system inertia calculation using wide area measurements. International Journal of Electrical Power and Energy Systems, 109. pp. 325-331. ISSN: 0142-0615

<https://doi.org/10.1016/j.ijepes.2019.02.013>

---

© 2019 Elsevier Ltd. All rights reserved. Licensed under the Creative Commons Attribution-Non Commercial No Derivatives 4.0 International License (<https://creativecommons.org/licenses/by-nc-nd/4.0/>).

**Reuse**

This article is distributed under the terms of the Creative Commons Attribution-NonCommercial-NoDerivs (CC BY-NC-ND) licence. This licence only allows you to download this work and share it with others as long as you credit the authors, but you can't change the article in any way or use it commercially. More information and the full terms of the licence here: <https://creativecommons.org/licenses/>

**Takedown**

If you consider content in White Rose Research Online to be in breach of UK law, please notify us by emailing [eprints@whiterose.ac.uk](mailto:eprints@whiterose.ac.uk) including the URL of the record and the reason for the withdrawal request.

# On-Line Power System Inertia Calculation using Wide Area Measurements

M. Sun, Y. Feng, P. Wall, S. Azizi, J. Yu, and V. Terzija

***Abstract-*** Future developments in power systems, e.g. relatively larger generator sets, the virtual power plant and synthetic inertia concept and connection of generation assets over inverters, will cause the system inertia to vary significantly. During system operation, if the inertia of the system is significantly lower than anticipated at the planning stage, then the existing, deterministic protection and control may fail to ensure system stability. Therefore, the ability to accurately determine the inertia of individual system areas, and the system as a whole, online would be very useful. In this paper, an Inertia Calculation Application (ICA), which could be implemented as part of a Wide Area Monitoring Protection and Control scheme, is presented. The necessary wide area measurements must be processed during large disturbances to the active power balance of the system. The ICA has been validated by using computer simulations, under laboratory conditions and by using real-life data recorded by a transmission system operator.

***Index Terms*** — Electro-mechanical transient processes, frequency, inertia, swing equation, WAMPAC, nonlinear estimation, power system measurement, power system transients, testing.

## 1. Introduction

The electrical power industry is entering a time of great change and innovation. Many of these changes and innovations have the potential to have a significant impact on the provision of frequency control within a power system. The introduction of large quantities of Renewable Energy Sources (RES), like wind power, that are intermittent and cannot produce electricity on demand will undermine the availability of generation reserves and frequency control services. In addition, much of the generation capacity provided by RES will offer little or no inertia to the system, as the majority of these energy resources will be connected to the system via DC links, causing the total system inertia to be dramatically reduced [1].

The loss of generation reserves that is associated with the use of RES based generation will occur at a time when the introduction of EPR<sup>TM</sup> nuclear reactor technology [2] will increase the size of the largest generator, and therefore the largest single contingency, in a system to over 1.6 GW.

However, the effects of the coming changes and innovations in the power industry are not all negative. The Global Positioning System (GPS) facilitated the introduction of Synchronized Measurement Technology

(SMT) [3], [4]. SMT allows system wide measurements to be used for real time protection and control actions through Wide Area Monitoring, Protection and Control (WAMPAC) applications.

The presence of large numbers of Plug-in Hybrid Electric Vehicles (PHEV) and other energy storage devices on the network will offer novel opportunities to support frequency control. However, use of PHEVs for frequency control, will reduce the total system inertia even further.

Many of the anticipated developments in power systems will significantly affect the response of the system frequency to a disturbance. The intermittent nature of these technologies will mean that their effects will also be intermittent; causing the frequency response to vary significantly throughout the day.

The combination of these factors, and others, will cause the inertia of a power system to vary significantly, both with time and location. For example, in a part of the system with high penetration of intermittent RES the inertia will be low when the relevant natural resources are unavailable, and will be high when they are, particularly if synthetic inertia is implemented.

The use of system loads, such as PHEV, to provide frequency control services will cause the availability of these services to vary with factors, such as domestic electricity prices, which transmission system operators do not control.

Contemporary electrical power systems are protected from dangerous under frequency conditions by deterministic Low Frequency Demand Shedding [5], commonly known as *under frequency load shedding* (UFLS). Existing UFLS schemes have each stage of shedding deterministically designed in advance, based on thorough system studies. Therefore, this deterministically designed frequency control may prove to be unsuitable, or even incapable, of offering efficient and secure protection in a future where the frequency response of a system will be highly variable.

These challenges will mean that the existing deterministic under frequency protection may need to be significantly changed by using the next generation of Information and Communication Technology (ICT) and Synchronized Measurement Technology to provide novel and adaptive solutions.

The current trend toward the increasing use of wide area measurement devices [4], [6] means that system data with reliable time stamps and a high sampling rate (each 20 ms) will be available to control centers in real time from across the entire system.

The focus of this paper is to present a new *Inertia Calculation Application* (ICA) supported by synchronized wide area frequency and active power measurements recorded from across the entire system. The ICA is intended to calculate the generator inertia available in individual system locations, to produce a profile of the inertia available in the system as a whole, after a disturbance has occurred using a methodology based on the

swing equation. Knowledge of the different levels of inertia that are across the system could allow under frequency protection to be adjusted on line to accommodate the random and uncontrolled variations in a systems frequency response that may occur in the future. The ICA can be classified as a novel WAMPAC application. It can be used as an enabler of other advanced WAMPAC applications, particularly those related to Wide Area Protection and Control, e.g. UFLS [7], or Smart Frequency Control (frequency control in low inertia systems) [8].

Previous work regarding the estimation of system inertia is limited to only a few papers. In 1997 Inoue et al. [9] used a swing equation-based method to estimate the inertia of the 60 Hz system in Japan. The focus of this work was modelling the frequency response of spinning reserve. This work dealt with  $M$ , the coefficient of inertia [10] or mechanical starting time [11], where  $M=2H$  and  $H$  is treated as the inertia constant in this paper. The estimation procedure used was based on the known size (in MW) of ten disturbances and the frequency transients measured at a single location in the power system.

In 2005 Chassin et al. [12] attempted to identify a link between the system inertia, estimated using the swing equation, and the system load. Estimates of  $M$  were made using post-mortem data regarding the disturbance size, and the frequency during the disturbance measured at a single location.

The work presented in [9] and [12] was performed off-line and used data recorded from only a single location to calculate the inertia of the entire system. This differs from the ICA quite significantly, this is because the intent of the ICA is to allow a profile of the inertia available across the system to be calculated immediately after a disturbance has occurred, rather than calculate a single value that represents the total inertia of the system.

The calculation of a single inertia value for the entire system is acceptable in a strong transmission system with relatively consistent inertia, where consequently the system frequency demonstrates limited variation between locations, like those in contemporary operation. However, this approach fails to accommodate the significant variations in system inertia that are anticipated in future power systems. The approaches presented in [9] and [12] use a calculation method that is based on the swing equation, similar to that used in the ICA. However, there is one significant difference. This is that this previous work was performed before the advent of SMT and as such the estimates were made off-line and used the known size of the disturbance that had occurred to serve as the power imbalance in the equation. This practice will cause a consistent over estimation of the generator inertia, which will increase as the load on the system increases. This is because not all of the power imbalance created by the disturbance will appear at the terminals of the generators, as small quantities of the power imbalance will be absorbed by the other power system components with energy

stored within them, such as motors. This causes the size of the imbalance experienced by the generators in the system to be smaller than the imbalance originally created by the disturbance.

Instead of the known size of the disturbance the ICA uses the measured power imbalance from across the system to allow the generator inertia available in the different parts of the system to be accurately calculated.

In this paper, a new application for calculation of power system inertia is presented. It is based on synchronized wide area measurements of the frequency and active power. In Section II the inertia calculation application is presented. Section III presents a robust method to estimate the rate of change of frequency. Section IV provides the results of a thorough testing of the new method using computer simulations. In Section V the results of laboratory testing are presented. Finally, Section VI gives results of the validation of the new method using some real-life data.

## 2. Inertia Calculation Application

In this section, the Inertia Calculation Application (ICA) will be presented. The method is based on simultaneously measuring the frequency and active power after a disturbance. Here, disturbance refers to any event that creates a large and sudden mismatch between the generated and consumed active power.

A suitable approach for recording the necessary simultaneous measurements is a Wide Area Monitoring System (WAMS) based on SMT. The main building blocks of SMT are Phasor Measurement Units (PMUs), Data Concentrator(s) (DCs) and the communication infrastructure necessary for transferring data from the PMUs to the DCs [3]. A WAMS of this nature would have the generic architecture shown in Fig. 1. In Fig. 1,  $\mathbf{s}_i$  denotes the vector of necessary information transferred from every installed PMU to the central DC, in which the ICA is computationally executed. Each of these vectors  $\mathbf{s}_i$  ( $i = 1, \dots, N$ , where  $N$  is the number of generators connected to the system) contains time stamped frequency and active power measurements from the PMU installed at the terminals of the  $i$ -th generator. The purpose of the data contained in the vector  $\mathbf{s}_i$  will be explained in detail in the method definition in Subsection II.B.

The starting point for development of the ICA is the modelling of the generators' behaviour immediately after a disturbance. This behaviour can be expressed using the inertia constant of a generator and the well-known generator *swing equation* [10], [11].

### A. Definition of the generator inertia constant

The generator inertia constant,  $H$ , is defined as the time that a generator can generate a specified amount of power, usually rated power or a selected base power, when operated at rated speed. Therefore, the inertia constant can be calculated using the following formula [10], [11]:

$$H = \frac{1}{2} \frac{J \omega_{sm}^2}{S_{base}} \quad (1)$$

where  $J$  is the total moment of inertia in  $\text{kg.m}^2$ ,  $\omega_{sm}$  is the rated mechanical speed in  $\text{rad/s}$ , and  $S_{base}$  is the selected base apparent power in MVA. In the case where there are multiple generators, if the rated power of a generator is used in (1), instead of a common base apparent power  $S_{base}$ , and the generators have different ratings then the inertia constant of each generator must be recalculated using a common base apparent power before they can be used in calculations.

### B. ICA Execution

The ICA must be initialized immediately after detecting a disturbance. Two consecutive sets of  $N$  measurement vectors,  $s_i$ , serve as the input for the ICA.

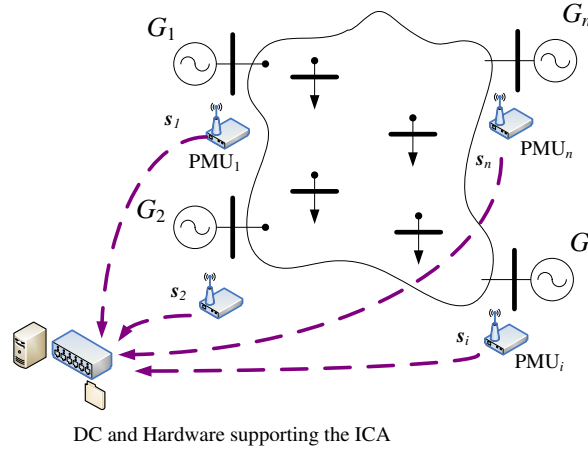


Fig. 1. A generic WAMS architecture that could support the ICA.

The starting point for the development of the ICA is the generator swing equation (2), which defines the relationship between the power imbalance,  $\Delta p_i$ , and electrical frequency,  $f_i$ , at the terminals of a single generator,  $i$ , immediately after a disturbance.

$$\frac{2H_i}{f_n} \frac{df_i}{dt} = p_{mi} - p_{ei} = \Delta p_i \quad (2)$$

where  $H_i$  is the inertia constant of that generator in seconds,  $df_i/dt$  is the rate of change of the electrical frequency at the terminals of the  $i$ -th generator in  $\text{Hz/s}$ ,  $f_n$  is the system nominal frequency in  $\text{Hz}$ ,  $p_{mi}$  is the mechanical power generated by the  $i$ -th generator in p.u.,  $p_{ei}$  is the electrical load at the terminals of the  $i$ -th generator in p.u. and  $\Delta p_i$  is the power imbalance at the terminals of the  $i$ -th generator in p.u.

If the instant of the disturbance is known, and the size of the power imbalance and rate of frequency change associated with the disturbance are available, the unknown inertia constant can be directly determined from (2) as below

$$H_i = \Delta p_i f_n / 2 \frac{df_i}{dt} \quad (3)$$

Equation (3) is only valid immediately after a disturbance, a time referred to as  $t=0^+$ . After this time other factors, not accounted for in equation (3) (e.g. generation unit controls, load response, series compensation, storage, spinning reserve, HVDC, AGC, LFC), begin to affect the dynamic behaviour of the system.

The rate of frequency change used in (3) can be determined using two consecutive frequencies measurements:

$$\frac{df_i}{dt} = \frac{f_i(t^+) - f_i(t^-)}{t_i^+ - t_i^-} \quad (4)$$

where  $f_i(t^+)$  is the frequency in Hz sampled after the disturbance;  $f_i(t^-)$  is the frequency in Hz sampled before the disturbance;  $t^-$  and  $t^+$  represent the times of the measurements before and after the disturbance, respectively. All of these values refer to the  $i$ -th generator. In order to achieve an accurate measurement of the rate of frequency change, the measurements must be made at a sufficiently high sampling frequency. In our approach, introduced in the next section, we concluded that the acquisition of frequency measurements once every cycle, e.g. a sampling frequency of 50 Hz for a 50Hz system, would satisfy the accuracy requirements for the ICA. A sampling frequency of this size is well within the capabilities of modern PMUs based on multiprocessor hardware platforms.

The power imbalance,  $\Delta p_i$ , used in (3) is defined in terms of mechanical and electrical power. However, the power imbalance can be redefined solely in terms of electrical power considering the following properties of a power system: a) mechanical power changes slowly when compared to electrical power and b) frequency control balances the mechanical and electrical power within the generator so they are approximately equal before a disturbance. These properties allow the electrical power measurements made before the disturbance to be used instead of mechanical power in the power imbalance definition (i.e.  $p_{mi} \approx p_{ei}(t^-)$ ). In conclusion, the power imbalance for the  $i$ -th generator,  $\Delta p_i$ , in (3) can be determined by using the following formula:

$$\Delta p_i \approx p_{ei}(t^-) - p_{ei}(t^+) \quad (5)$$

where  $p_{ei}(t^+)$  is the electrical power measured after the disturbance in p.u. and  $p_{ei}(t^-)$  is the electrical power measured before the disturbance in p.u.

Equations (3)-(5) allow the inertia constant of the  $N$  generators in the system to be calculated using only the data contained in the two sets of  $N$  measurement vectors,  $\mathbf{s}_i$ , provided by the supporting SMT.

If a generator is disconnected from the system it is important that it is excluded from the ICA, as it no longer forms part of the system response. The exclusion of measurements from a disconnected generator can be achieved by defining a binary variable  $o_i$ . This variable is set to 1 if a generator is connected and 0 if it is not. This variable does not necessarily need any additional information from the system as the existing measurements could be used to determine the status of the generator.

The system,  $H_{SE}$ , can now be calculated as a sum of the individual inertia constants,  $H_i$ , of all the generators connected to the system:

$$H_{SE} = \sum_{i=1}^N o_i H_i \quad (6)$$

where  $o_i$  is a binary variable that is 1 if the  $i$ -th generator is connected to the system and 0 if it is not. The inertia of each of the  $N$  individual generators,  $H_i$ , is estimated using (3).

The  $N$  generators referred to in this discussion could include every generator in the system, or only the generators in the specified areas the ICA is executed for.

### 3. Estimation of the Rate of Frequency Change

To estimate the unknown rate of frequency change estimation, the following linear frequency model was assumed:

$$z(t) = x_1 + x_2 t + \xi(t) \quad (7)$$

where  $x_1$  is the average frequency,  $x_2$  is the unknown rate of frequency change and  $\xi(t)$  is the random noise.

Assuming that the input signal is uniformly sampled with the sampling frequency  $f_s$  and the sampling period  $T_s = 1/f_s$ , the value of  $t$  at a discrete time index is given by  $t_k = kT_s$  and the following discrete representation of the signal model should be used:

$$z_k = x_1 + x_2 t_k + \xi_k, k = 1, \dots, p \quad (8)$$

where all unknown parameters in (8) now have the subscript  $k$ . The following matrix equation for all samples, belonging to the data window, can be established:

$$\begin{bmatrix} z_1 \\ \vdots \\ z_p \end{bmatrix} = \begin{bmatrix} 1 & T \\ \vdots & \vdots \\ 1 & pT \end{bmatrix} \begin{bmatrix} x_1 \\ x_2 \end{bmatrix} + \begin{bmatrix} \xi_1 \\ \vdots \\ \xi_p \end{bmatrix} \quad (9)$$

The system of linear equations (9) can be now presented as follows:

$$\mathbf{z} = \mathbf{H}\mathbf{x} + \boldsymbol{\xi} \quad (10)$$

By this, an overdetermined system of linear equation is obtained. It can be solved using the traditional Least Squares Method, which minimizes the sum of error squares:

$$\hat{\mathbf{x}} = (\mathbf{H}^T \mathbf{H})^{-1} \mathbf{H}^T \mathbf{z} = \mathbf{H}^\# \mathbf{z} \quad (11)$$

For  $p = 2$ , one directly obtains:

$$x_2 = \frac{\Delta f}{\Delta t} = \frac{z_2 - z_1}{T} \quad (12)$$

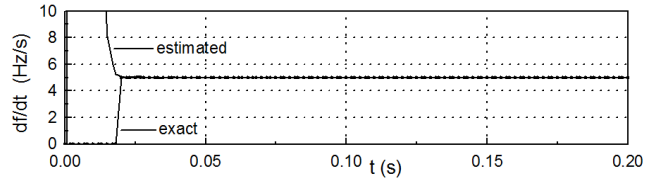


Fig. 2. Estimated test signal rate of frequency change.

To demonstrate how the above numerical algorithm for estimation of unknown rate of frequency change works, let us assume a sinusoidal test signal with an artificial frequency step change from 50 Hz to 55 Hz at 0.02 s and further constant frequency change 5 Hz/s. Let us also assume that the frequency has been measured using one of existing algorithms, e.g. [13], [14]. By setting data window size for the rate of frequency estimation to 20 ms, the rate of frequency change presented in Fig. 2 is obtained. It is obvious that the method is suitable for processing of signals with even faster frequency changes compared to those encountered in real power systems.

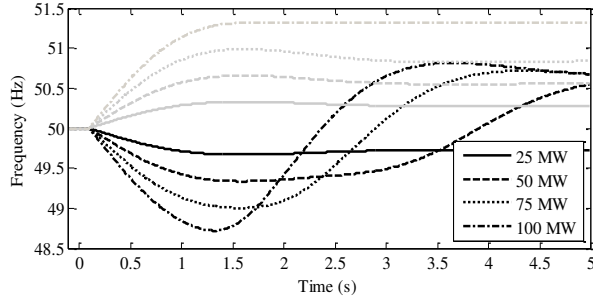


Fig. 3. Frequencies for a single-machine test system; the black and grey lines denote a load increase and decrease respectively.

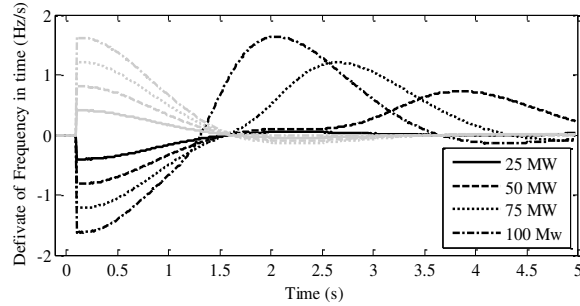


Fig. 4. Frequency derivatives for a single-machine test system, the black and grey lines denote a load increase and decrease respectively.

From the perspective of practical application of the any numerical algorithm for measurement of the  $df/dt$ , one has to consider a very high sensitivity to the quality of frequency measurement. The actual power system frequency varies in a very narrow range, for example  $\pm 0.5\text{Hz}$ , which is the *statutory limit* in GB power system. Consequently, the  $df/dt$  measurement is quite a challenging task, particularly if the measured frequency contains noise. Using larger data window sizes, the accuracy of  $df/dt$  measurement can be improved but causing this unacceptably long delay in any application relying on  $df/dt$ . That is why the quality of frequency measurement must be as better as possible, so that the data window size can be shortened, allowing the application to response faster.

#### 4. ICA Testing and Validation Through Computer Simulated Tests

The behavior of the ICA presented in this paper can be investigated through computer based dynamic simulations of power systems of different complexity. For this purpose, two test systems were used:

The *first test system* consists of a single synchronous generator connected directly to a static constant power load. This test system is used to demonstrate the proper behavior of the method in the simplest case of inertia estimation. Disturbances are created using load step changes, representing both load increases and decreases.

The *second test system* consists of a 3-machine power system. This test system is used to test the behavior of the ICA in a multi-machine system, for different types and size of disturbances. Simulations performed using

this system will give some indication of the influence of various system properties on the reliability of the ICA.

The frequency response of both test systems was simulated using DIgSILENT™ PowerFactory® [15]. The ICA execution was implemented in MATLAB.

#### A. Single-machine Test System Case

The single-machine test system consists of a gas turbine generation unit connected directly to a single static load. The unit is rated as a 210 MVA, 50 Hz synchronous generator with an inertia constant of 7.334 s on a 210 MVA base. The load has a constant power consumption of 100 MW and 50 MVar. The active power demand was step changed by  $\pm 25$ ,  $\pm 50$ ,  $\pm 75$  and  $\pm 100$  MW to provoke system frequency changes. Note that negative values denote a reduction in load. Fig. 3 and 4 show the frequency response and the derivative of this frequency for these load changes in the single-machine test system.

Table 1 Inertia Calculation Errors for The Single-Machine Test System

$\Delta p$ (MW)	$df/dt$ (Hz/s)	$H^{est}$ (s)	Error (%)
-100	-1.62	7.34861	0.05
-75	-1.208	7.3912	0.64
-50	-0.8121	7.32961	-1.96
-25	-0.4059	7.33232	-0.16
+25	0.4059	7.33232	-0.16
+50	0.8121	7.32961	-1.96
+75	1.208	7.39120	0.64
+100	1.62	7.34861	0.05

The shapes of the frequency response curves are different for a step increase and decrease in the load. This is due to the characteristics of the generator controller and its growing influence over the frequency response within a few seconds of the disturbance occurring. This difference in frequency behavior will have no influence on the behavior of the ICA as the frequency measurements used are taken before this controller action occurs.

The curves of the derivative of frequency are shown in Fig. 4. It is evident that larger load changes produce larger excursions in the rate of change of frequency.

Table 1 shows the calculated inertia ( $H_{est}$ ), produced by the ICA for different load step changes ( $\Delta p$ ) and relative errors. It is noticeable in Table I that the derivative of the frequency at  $t = 0^+$  is of the same magnitude

for a load increase and decrease of the same size, with the only difference in the two data values being that the signs are inverted. The errors obtained are negligible from a practical viewpoint. The maximum error in the inertia estimation is for load changes of  $\pm 50\%$  (the estimates produced for both a load increase and decrease were the same).

These results demonstrate two properties of the ICA: 1) The error in the estimate of the inertia is the same for load changes of the same size, regardless of whether changes represent a load increase or decrease; 2) The estimation method is generally reliable despite the variation in the disturbance size.

### B. Multi-machine Test System Case

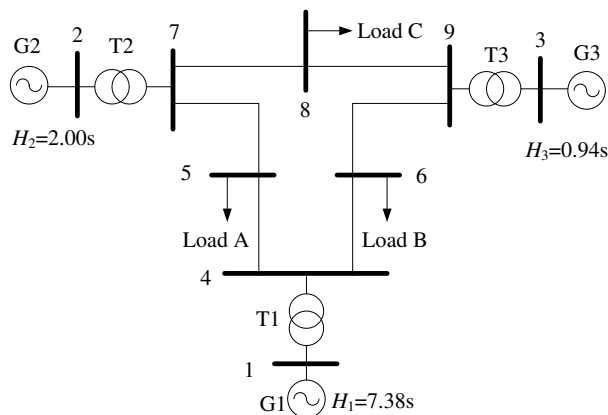


Fig. 5. Three-machine, 60 Hz test power system.

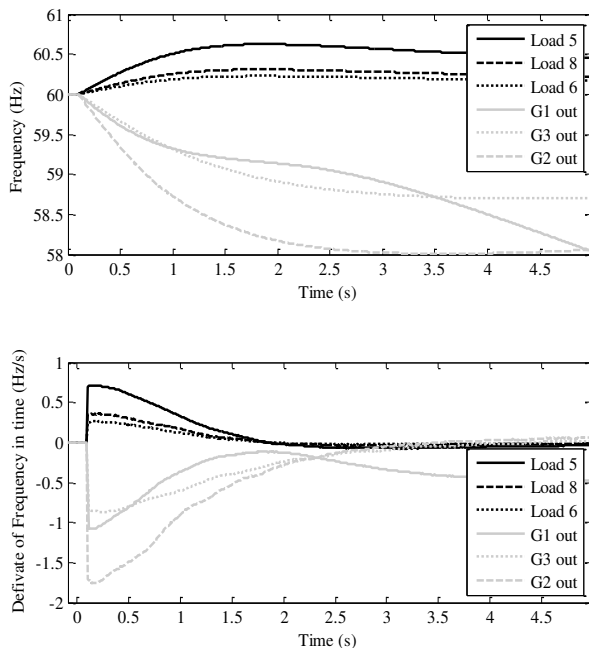


Fig. 6. Inertia Centre Frequency response for Test with the 3-machine tests system.

The multi-machine test system (see Fig. 5 and for a detailed description [16]) simulations were performed to determine if the properties identified in the single bus case held true for a more complex system, and to investigate the impact of network properties on the performance of the ICA.

The simulations performed consisted of load step changes at each load bus, using 25% steps like those used in the single bus case. In addition to these load change simulations, the inclusion of multiple generators allowed the simulation of sudden generator disconnection disturbances to be included. It is important to note, the systems net load of 320.2 MW, is used as the base,  $S_B$ , for the inertia estimates. A base conversion, from the individual generators ratings to the system base, gives the inertia of G1, G2, and G3 as 7.38 s, 2.00 s and 0.94 s, respectively.

Fig. 6 shows the equivalent system frequency, calculated using the frequency of the inertia center method, and its rate of change data for a single case of each disturbance considered (changes at Load A, B and C and outages of G1, G2 and G3). Note that the frequency of the inertia center is calculated as an inertia weighted sum of the frequency of each generator in the system, as described in [11], and represents the equivalent frequency behavior of the system.

In Fig. 6 it is noticeable that the system frequency for an outage of G1 is unstable, demonstrated by a second frequency decline at approximately 2.5 s. However, based on comparison of the estimate errors seen in Table II the systems instability has not compromised the performance of the estimation method. This is not surprising given the fact that the instability occurs after the disturbance and, therefore, after the moment the data used by the ICA was collected but it is a vital property of the ICA as it will allow the inertia estimates to contribute to adaptive actions that could prevent this instability.

Table 2 Estimation Results of Inertia of the 3-machine test System

Event	$\Delta p$ (MW)	$H_{actual}$ (s)	$df_c/dt$ (Hz/s)	$H_{estimated}$ (s)	Error (%)
Gen 1 out	-71.64	2.98730	-1.07025	2.97238	0.49952
Gen 2 out	-163.00	8.45426	-1.67206	8.55272	-1.16470
Gen 3 out	-85.00	9.53044	-0.83390	9.39125	1.46055
Load A	80.00		0.68824	10.55725	-0.67951
Load B	40.00	10.48600	0.25385	10.46730	0.17829
Load C	30.00		0.33891	10.75954	-2.60867

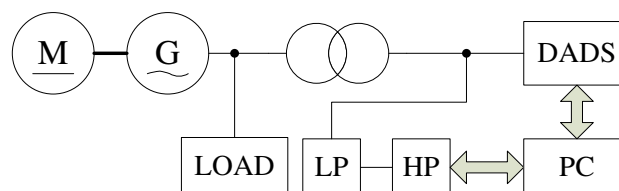


Fig. 7. Setup used in laboratory testing, consisting of a Motor-Generator set, Data Acquisition Digital System and a load made up of 75W blocks.

The results in Table 2 show that the ICA can be used to produce reliable estimates of system inertia regardless of the magnitude of the system inertia. This can be stated Table 2 based on because the disconnection of a generator changes the systems inertia, at the moment of its disconnection, so the system inertia for the data collected at  $t=0^+$  is only dependent upon the remaining, connected, generators. The new system inertia for each generator disconnection is given in Table 2. It is clear that the errors obtained do not vary in an extreme way for the four different values of system inertia seen in Table 2.

## 5. Laboratory Testing

In order to confirm the validity of the ICA, the laboratory setup depicted in Fig. 7 has been prepared [14]. The calculations presented here used a power base of 100 W and a frequency base of 50 Hz.

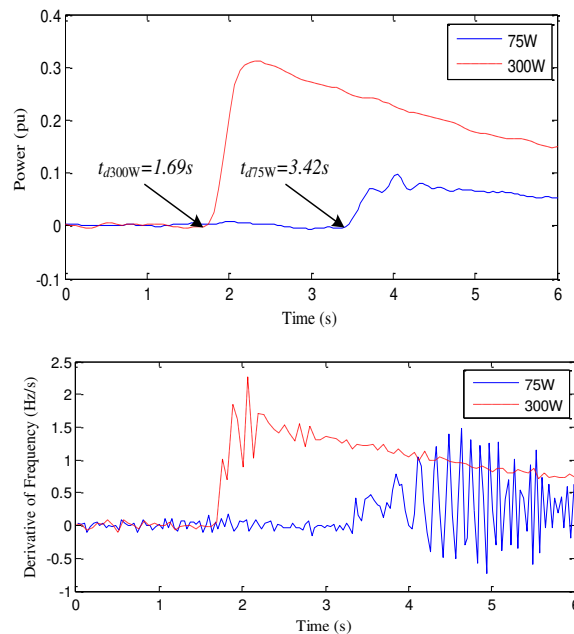


Fig. 8. Power and derivative of frequency data for Test 1 and 2, load decreases of 300W and 75W respectively.

Table 3 Estimation Results of Inertia Laboratory Test System

Test	$\Delta p$ (W)	$t_{\text{outage}}$ (s)	$df/dt$ (Hz/s)	$H^{est}$ (Ws)	$\Delta p^{est}$ (W)
1	300.0	2.34	1.60	4.6875	-
2	75.0	3.76	0.40	-	75.0

Data records have been obtained from the Motor-Generator Set (M-G Set). The generator output voltage was transformed to a suitable voltage level and then digitized by using a Data Acquisition Digital System - DADS (12-bit-A/D converter with sampling frequency  $f_s=1600$  Hz). To provide precise frequency measurements a HP 3457A Multimeter (HP) was used. This device was connected to the circuit over a low-pass analog filter (LP) with a cut-off frequency of 125.0 Hz. Both the HP and DADS were connected to a Personal Computer

(PC) through an IEEE-488-Bus. Before the disturbance, the M-G Set was operated in a steady-state with the frequency maintained at approximately 50.1 Hz.

In order to demonstrate the validity of the ICA, two tests have been designed:

- Test 1 consisted of a sudden disconnection of 300 W of resistive load from the M-G set.
- Test 2 consisted of 75 W of resistive load being suddenly disconnected

Fig. 8 shows the results of Tests 1 and 2. Starting from steady state conditions, a sudden disconnection at  $t=2.34$  s of 300 W of resistive load from the M-G set resulted in a rapid increase in frequency. The rate of change of frequency was approximately +1.60 Hz/s.

The frequency response and derivative of this frequency for a sudden disconnection of 75W of resistive load from the M-G set at 3.76 s is shown in Fig. 7. The frequency increases as a consequence of the power imbalance at approximately +0.40 Hz per second. Considering the algorithm presented in this paper, the power imbalance in Tests 2 can be estimated based on the inertia estimate from Test 1 and the derivative of the frequency seen in Test 2. The result of the estimate can be seen in Table III.

Using the Test 1 estimated inertia and the derivative of frequency recorded in Test 2 results in an estimated power imbalance of 75.0 W. When this result is compared with the actual power imbalance, it indicates that, in this case, the estimation obtained from this algorithm has no error. This demonstrates that it is acceptable to use two disturbances for which the system inertia was the same, but unknown, to verify the execution of the ICA.

## 6. Real-Life Testing

Once the proper behavior of the ICA was validated through M-G set tests and dynamic simulations, the ICA was applied to frequency and power data records obtained from real power systems.

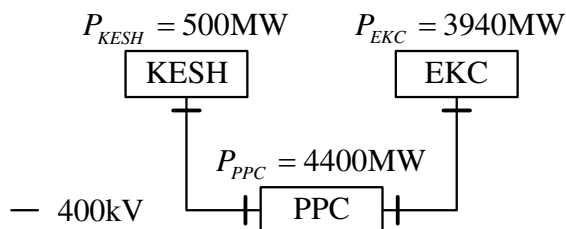


Fig. 9. Real Test System A: EKC (Power systems of Serbia, Macedonia and Montenegro), PPC (Power System of Greece) and KECH (Power system of Albania).

This data was recorded from only a single location, in contrast to the proposed ICA execution. However, the strong nature of contemporary power systems, from which this data was recorded, means that it is valid to assume that the frequency is consistent across the entire system.

These real data tests focused on estimating the inertia of the whole system. The exact value of this inertia was unknown and, therefore, the method could not be directly evaluated by comparing an estimate and a true value. Instead, the operation of the method was evaluated in the following way. Firstly, an estimate for the total inertia was made for one disturbance. This inertia estimate was then used to estimate the magnitude of the power imbalance ( $\Delta p$ ) in the next, or second, disturbance. However, the actual value of the power imbalance in this second disturbance was known and could therefore be compared to the estimated result. In this way, the estimated system inertia was implicitly validated.

This approach is valid provided that the system inertia was similar (or ideally the same) for the two disturbances considered, as shown in section IV. Ideally, the data available for a period of time would contain two disturbances and it could be, therefore, assumed that the second disturbance does not cause a significant change in the inertia of the system due to the large number of generators seen in a real network.

Since September 21<sup>st</sup>, 1991 (04:50pm) the Electrical Power System of Serbia (EPS) has been operating as an isolated power system, disconnected from the Union for the Co-ordination of Transmission of Electricity (UCTE) grid, and connected only to the Greek, Albanian, Montenegrin and Macedonian networks, in the configuration shown in Fig. 9. The estimation method described in this paper was applied to one pairs of disturbances for this network.

#### *1) Generator disconnection followed by a load disconnection*

The following real network data was collected during a planned disturbance on October 20<sup>th</sup>, 1993 when at 10:01:14.78 a.m. 200 MW of generation from the Bajina Bašta Hydro Power Plant in the Republic of Serbia was disconnected. Before the disturbance, the interconnected system operated in a steady-state and was supplying approximately 8,840 MW. The power transfer between the three areas was approximately zero. The system frequency was maintained at 50.02 Hz. The voltage samples were acquired using a Data Acquisition Digital System (12-bit-A/D converter with sampling frequency 500 Hz) installed at the Control Centre in Belgrade, Serbia. Frequency and rate of change of frequency were estimated from the generators output voltage by using the non-recursive NTA algorithm and the Least Error Squares algorithm, respectively, as described in [17], the results of which are given in Fig. 10.

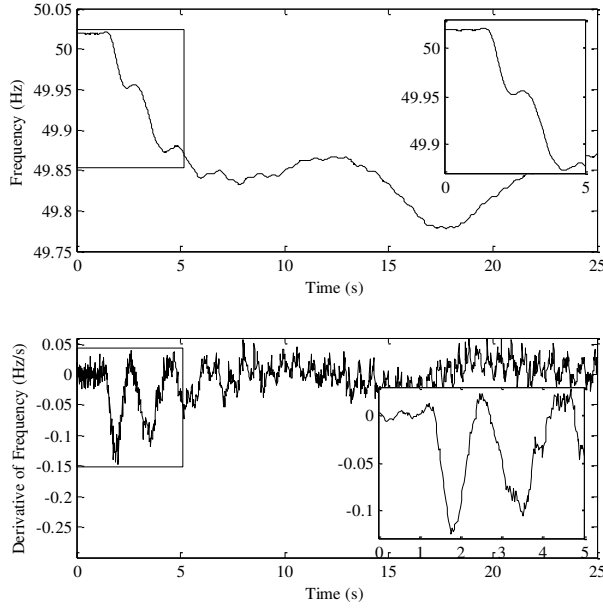


Fig. 10. Frequency and derivative of frequency data for the disturbances

Immediately after the disturbance, the frequency declined quickly. Application of the method presented in this paper, using a value of  $-0.125$  Hz/s for the derivative of the frequency and the known size of 200 MW for the disturbance, gave an estimate for the inertia of the entire power system as  $H^{est} = 4.5200$  s, when the approximate system load of 8,840 MW was used as a power base.

## 2) Load disconnection in Macedonia

The second disturbance consisted of a portion of customers in Macedonia (approximately 40 MW) being disconnected. As seen in Fig. 10 this caused a temporary frequency increase (between 9 s and 14 s) at a rate around  $+0.02$  Hz/s. By combining this value with the system inertia estimated during the generator outage gave the power imbalance estimate of 34.87 MW. The estimation error was about 12.8%.

## 7. Conclusion

This paper shows that the new *Inertia Calculation Application (ICA)*, based on wide area measurements, can be used to accurately calculate the system inertia on-line. From the results presented in Section IV it is evident that the accuracy of the power system inertia estimates is independent of the type, size, and location of the disturbance during which the necessary data is gathered. The computer simulated testing of the ICA has shown that it is accurate and reliable. The motor-generator set and real-life power system measurement-based testing have shown that the accuracy of the ICA is also acceptable when the calculation is based on laboratory and real-life data. This system inertia information would be useful for system operators

working in an environment where changes to the nature of large power systems (e.g. a high penetration of intermittent generation) had caused the system inertia to become quite variable and potentially reduced to a level where system security may be compromised. The ICA is also capable of producing accurate estimates of the inertia of individual generators, or parts of the system. Authors are currently exploring options for implementing the ICA into novel Wide Area Protection and Control applications.

## 8. References

- [1] R. J. Best, C. F. Ten, D. J. Morrow, and P. A. Crossley, "Synchronous island control with significant contribution from wind power generation," *Integration of Wide-Scale Renewable Resources Into the Power Delivery System, 2009 CIGRE/IEEE PES Joint Symposium* , pp.1-1, 29-31 July 2009.
- [2] A. Teller, "The EPR Reactor: Evolution to Gen III+ based on proven technology", Areva, Feb. 2010.
- [3] V. Terzija, G. Valverde, D. Cai, P. Regulski, V. Madani, J. Fitch, S. Skok, M. Begovic, A. Phadke, "Wide-Area Monitoring, Protection, and Control of Future Electric Power Networks," *Proceedings of the IEEE* , vol. 99, no. 1, pp.1-14, Jan. 2011.
- [4] A. G. Phadke and J. S. Thorp, "Synchronized phasor measurements and their applications", Springer Verlag, 2008.
- [5] V. Terzija, "Adaptive Underfrequency Load Shedding Based on the Magnitude of the Disturbance Estimation", *IEEE Transactions on Power Systems*, Vol. 21, No. 3, Aug. 2006, Page(s): 1260- 1266.
- [6] S. Chakrabarti, E. Kyriakides, B. Tianshu Bi; D. Cai, and V. Terzija, "Measurements get together," *IEEE Power and Energy Magazine*, vol.7, no.1, pp.41-49, Jan.-Feb. 2009.
- [7] "H2020 Migrate", *H2020-migrate.eu*, 2018. [Online]. Available: <https://www.h2020-migrate.eu/>. [Accessed: 01- Sep- 2018].
- [8] National Grid, "SMART Frequency Control project | National Grid", *Nationalgridconnecting.com*, 2018. [Online]. Available: [http://www.nationalgridconnecting.com/The\\_balance\\_of\\_power/](http://www.nationalgridconnecting.com/The_balance_of_power/). [Accessed: 01- Sep- 2018].
- [9] T. Inoue, H. Taniguchi, Y. Ikeguchi and K. Yoshida, "Estimation of Power System Inertia and Capacity of Spinning-reserve Support Generators Using Measure Frequency Transients", *IEEE Transactions on Power Systems*, Vol. 12, No. 1, February 1997
- [10] J. Machowski, J. Bialek, and J. Bumby, "Power System Dynamics and Stability" 2<sup>nd</sup> ed. , Hoboken, NJ: John Wiley & Sons, 2008, ch 5, sec 5.1, pp 169-172.
- [11] P. Kundur, "Power System Stability and Control", New York: McGraw-Hill, 1994. ch 3, sec 3.9
- [12] D. P. Chassin, Z. Huang, M. K. Donnelly, C. Hassler, E. Ramirez and C. Ray, "Estimation of WECC System Inertia Using Observed Frequency Transients", *IEEE Transactions on Power Systems*, Vol. 20, No. 2, May 2005.
- [13] V. Terzija, M. Djurić, and B. Kovačević, "Voltage Phasor and Local System Frequency Estimation Using Newton Type Algorithm," *IEEE Trans. on Power Delivery*, Vol.9, No.3, Jul. 1994, pp.1368-1374.
- [14] V. Terzija, M. Djurić, and B. Kovačević, "A New Self-Tuning Algorithm for the Frequency Estimation of Distorted Signals", *IEEE Trans. on Power Delivery*, Vol.10, No.4, Oct. 1995., pp 1779-1785.

- [15] "DigSILENT Solutions PowerFactory Software", *IEEE Power and Energy Magazine* [Online], Issue: Sept-Oct 2006,  
Available: <http://ieeexplore.ieee.org/stamp/stamp.jsp?tp=&arnumber=1687801>
- [16] P. M. Anderson, and A. A. Fouad, " Power System Control and Stability," The Iowa Press, Ames, 1977.
- [17] V. Terzija, V. Stanojevic, M. Popov and L. van der Sluis, "Digital Metering of Power Components According to IEEE Standard 1459-2000 Using the Newton-Type Algorithm," in *IEEE Transactions on Instrumentation and Measurement*, vol. 56, no. 6, pp. 2717-2724, Dec. 2007.